Monte Carlo study of the statistics of electron capture by shallow donors in silicon at low temperatures

A. Palma,* J. A. Jiménez-Tejada, A. Godoy, J. A. López-Villanueva,† and J. E. Carceller
Departamento de Electrónica y Tecnología de Computadores, Facultad de Ciencias, Universidad de Granada, 18071 Granada, Spain
(Received 28 November 1994; revised manuscript received 30 January 1995)

A statistical study of electron capture by shallow donors in silicon without an electric field as a function of temperature and impurity concentration is presented. The Monte Carlo calculations (based on the cascade capture theory) of the times spent by carriers in the conduction band before falling into impurity centers (i.e., the capture times) show evidence of nonexponential capture kinetics behavior. This work has allowed us to interpret the slow time decay of the distributions of capture times as the capture time actually measured in experiments. We have achieved very good agreement between the capture cross sections calculated by our Monte Carlo simulation with the experimental ones and with a previous analytical model that provides asymptotic behaviors of the thermal capture cross section.

I. INTRODUCTION

Phonon-emission capture of carriers by shallow impurities in semiconductors has been widely studied since the 1950s.[1] The cascade model originally introduced by Lax[2] and further elaborated on by the Leningrad group[3] is traditionally used to explain these phenomena. One of the more important drawbacks of these analytical approximations, however, was the calculation of the so-called sticking probability, defined as the probability of a carrier reaching the ground state of the impurity levels without going back to the conducting band.

A method for studying carrier capture by the cascade process in a Monte Carlo simulation was proposed by Reggiani *et al.*[4,5] for *p*-type Si doping. They avoided the problem of evaluating the sticking probability because the reemission processes are consistently accounted for in the simulation. In a previous work,[6] we applied this method for *n*-type Si. However, one fundamental question is still unclear: the exact reproduction of the experimental behavior of the capture cross section vs temperature. To clarify this point, we present the results of a statistical study of nonradiative carrier capture by shallow-donor impurities in silicon at low temperatures, in the absence of an electric field. The study has been performed using the Monte Carlo method in which, in addition to the lattice-scattering processes, the capture process has been included in semiconductor transport by the perturbation induced by the Coulombic potential of the attractive center. The absence of external electric field and the range of temperatures studied have allowed us to use a semiclassical treatment; a complete quantum treatment is necessary in samples under an electric field.[7] Our study has provided us with a unique and good agreement between the experimental capture cross sections and our numerical results at temperatures from 1 to 80 K.

This paper is organized as follows. In Sec. II an explanation of the Monte Carlo procedure is given. In Sec. III, we have analyzed the distribution of electrons with a given capture time interval, where the capture time is the mean time that a carrier spends in the band before falling down through the impurity states. In this section, we have interpreted two decay times associated with the statistics of the capture time. Finally, some conclusions are provided in Sec. IV.

II. MONTE CARLO SIMULATION

Due to the possibility of combining the scattering events in the semiconductor with the capture mechanism, the Monte Carlo method has demonstrated itself to be an ideal procedure for studing nonradiative capture mechanisms at a microscopic level.[4–7]

In the conventional Monte Carlo algorithm,[8] we simulated the motion of an electron in the space energy of the silicon conduction band perturbed by the Coulombic potential created by a random distribution of ionized impurities, N_D^+, as shown schematically in Fig. 1. In accordance with *Lax*,[2] we have considered that the high bound states of the center are very close to each other and, therefore, they can be introduced as a quasicontinuum of states. We have taken the minimum of this quasicontinuum to be the first excited state, E^1, produced by the potential.[3–5] We have assumed that E^1 is 11.5 meV below

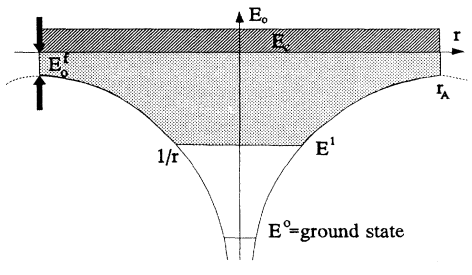

FIG. 1. Schematic representation of total space energy of the conduction band of silicon perturbed by the potential created by a Coulombic center. The ground level E^0 and the first excited state E^1 of the trap are plotted. The percolation energy E_0^f (corresponding to the limit of energy of the center influence in a randomly distributed concentration N_D^+) is also plotted.

the edge of the conduction band.[9] Therefore, within the temperature range $K_B T < E^1$ (K_B being the Boltzmann constant and T the lattice temperature), the semiclassical approach can be applied in the whole energy region covering the conduction band and the bound states.[3] In any event, as we will show, in our simulation the carrier does not reach energies lower than 1 meV below the band, a region where the continuum of energy is easily assumable.

With this scheme, the carrier kinetic energy E_k is equal to the total energy (or simply the energy) E_0 minus the potential one, $U(r)$:

$$E_k = E_0 - U(r) , \qquad U(r) = -\frac{e^2}{4\pi\epsilon r} , \tag{1}$$

where e is the electron charge and r the position relative to the impurity. Negative energy was assigned to the bound states. To reduce the simulation to the one-impurity range, both the energy-state density and the scattering probabilities, $P(E_0)$, were spatially averaged:

$$P(E_0) = \langle P(E_k) \rangle = \frac{\int_0^{r_m} P(E_k) r^2 dr}{\int_0^{r_A} r^2 dr} , \tag{2}$$

where $r_A = (N_D^+)^{-1/3}$ is the average semidistance between impurities in a sample with an impurity concentration of N_D^+ (this r_A is four times greater than the estimated semidistance to account for the percolation level[3-5]), and r_m is determined by the carrier energy: $r_m = r_A$ for $E_0 > -E_0^f$ and $r_m = -r_A E_0^f / E_0$ for $-E^1 < E_0 < -E_0^f$, with $E_0^f = e^2/4\pi\epsilon r_A$. E_0^f is the potential energy in $r = r_A$ (Fig. 1). Introducing the dimensionless distance $x = r/r_A$, Eq. (2) becomes:

$$\langle P(E_k) \rangle = 3 \int_0^{x_m} P\left[E_0 + \frac{E_0^f}{x} \right] x^2 dx , \tag{3}$$

where if $E_0 > -E_0^f$, $x_m = 1$, and if $-E^1 < E_0 < E_0^f$, $x_m = -E_0^f / E_0$.

Handling the spatial variable x directly in the simulation implies the nonphysical problem of tracking the electron to very large kinetic energies when x tends to 0. Our procedure avoids this by eliminating the explicit numerical use of this variable. Assuming that all the relative positions to the center have the same probability,[5] we can work solely with the perturbed carrier energy. The idea is to find a value for an effective energy, ϵ_m, that plays the same role as the carrier energy in an unperturbed lattice but that takes into account the effects of the Coulombic potential. Equation (3) can in consequence be written as follows:

$$3 \int_0^{x_m} P\left[E_0 + \frac{E_0^f}{x} \right] x^2 dx = 3 P(\epsilon_m) \int_0^{x_m} x^2 dx = P(\epsilon_m) x_m^3 , \tag{4}$$

where no spatial dependence is explicitly observed. In any case, due to the energy dependence of the scattering mechanisms, the integral on the left-hand side of Eq. (4) has no singularities. In the cases of phonon-scattering mechanisms in silicon, the numerically calculated ϵ_m values were

$$\epsilon_m = \begin{cases} E_0 + \frac{4}{3} E_0^f , & E_0 > -E_0^f \\ \dfrac{|E_0|}{3} , & -E^1 < E_0 < -E_0^f . \end{cases} \tag{5}$$

Therefore, from Eqs. (4) and (5), the scattering probabilities were calculated as

$$P(E_0) = \begin{cases} P(E_0 + \frac{4}{3} E_0^f) , & E_0 > -E_0^f \\ \left[-\dfrac{E_0^F}{E_0} \right]^3 P\left[\dfrac{|E_0|}{3} \right] , & -E^1 < E_0 < -E_0^f . \end{cases} \tag{6}$$

All phonon-scattering mechanisms were included in the simulation of electron transport in the conduction band: acoustic phonons and both intervalley and intravalley nonpolar optical phonons. Elastic scattering was omitted since we are only interested in scattering involving a change of energy. The nonparabolic effect was included in Si, and the phonon energies and coupling constants were taken from Ref. 8.

In Fig. 2 the scattering probabilities by acoustic phonons, P_{ac}, for several donor concentrations at 5 K are shown. The plot includes the negative-energy region corresponding to the quasicontinuum of bound states, where the probabilities are not null. In this region, we can also appreciate an increase of the probabilities with the impurity concentration; this dependence is included in energy E_0^f.

The energies of the acoustic phonons are also perturbed by the presence of the Coulombic potential. In order to prevent the electron from descending below $-E^1$ and penetrating into the region of forbidden energies, we used an average value $\epsilon_m = (E^1 + E_0)/3$ to calculate the phonon energy in the range $-E^1 < E_0 < -E_0^f$, and the same value as in Eq. (5) when $E_0 > -E_0^f$.

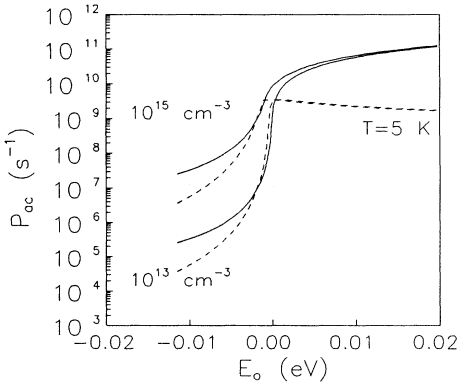

FIG. 2. Acoustic scattering rates as a function of the carrier energy in n-type Si for a temperature $T = 5$ K. Solid and dashed lines refer to the processes of phonon emission and absorption, respectively. The pairs of curves are calculated for an ionized donor concentration of $N_D^+ = 10^{13}$ and 10^{15} cm^{-3}.

In this context, initially, the thermal energy was assigned to the carrier before introducing the changes caused by the centers, and it was allowed to move in an unperturbed lattice, to avoid possible influence from the initial state. Once the perturbation is introduced, the electron can evolve through the bound and band states, according to the probabilities and phonons defined above, until it is captured. Thus, the physical magnitudes recorded for the electron were its mean velocity $\langle v \rangle$ and its capture time τ_c which needs to be defined.

Until now, the capture time τ_c was defined as the total time the carrier spends in the band divided by the number of transitions to the excited-state region.[4,5] In order to stop the simulation of one electron, it is necessary to define a cutoff energy E_{coff}. We chose E_{coff} as a multiple of $-K_B T$. In accordance with this definition, two types of transitions, and two capture times, can be analyzed: transitions causing an electron to go below E_{coff} and transitions making an electron go below zero energy and then rise without reaching the level E_{coff}. When the electron reaches the level E_{coff}, two capture times are recorded: the total time spent in the band, τ_{c2}, and the ratio between this time and the number of crossings by the zero energy, n. This capture time τ_{c1} is defined as

$$\tau_{c1}=\frac{\tau_{c2}}{n} . \tag{7}$$

This procedure is repeated for N electrons, with N being a value large enough to obtain an acceptable distribution of capture time and mean velocities. The averages of the capture times, τ_{c1} and τ_{c2}, and the average of the mean velocities, $\langle v \rangle$, are obtained. Therefore the average capture cross section σ_c is calculated as follows:

$$\sigma_c=\frac{1}{\tau_c N_D^+ \langle v \rangle} , \tag{8}$$

where τ_c takes the values τ_{c1} or τ_{c2} with two different average cross sections σ_{c1} and σ_{c2} being obtained, respectively.

The behavior of the average cross sections for the capture of electrons by shallow-donor impurities in n-type Si is shown in Fig. 3. The simulations were done with a cutoff energy of $E_{\text{coff}}=-K_B T$. The two curves shown in the figure correspond to σ_{c1} (solid line) and σ_{c2} (dashed line). Experimental data available in the literature referring to shallow donors P, As, and Sb in silicon[10–12] have also been plotted for comparison. It is clear from this figure that there is a certain imprecision in the definition of the capture time, which we have attempted to remove in this study.

III. RESULTS

Once the capture time has been evaluated with the simulation of N identical electron-impurity systems, the statistical distribution of the capture times, τ_{c1}, can be analyzed. We calculated the histograms of the number of electrons, N_c, with a given capture-time interval.

The distribution of N_c displays a double exponential decay, as shown in Fig. 4. The two time constants can be extracted: τ_s for the short-time decay and τ_1 for the long-time decay. The histograms of N_e for different shallow-donor concentrations at 30 K are plotted in this figure. This result is similar to that reported in Ref. 13, but our Monte Carlo calculations have allowed us to give a definition of the capture time, which has allowed us to reproduce the thermal dependence of the experimental data of the electron capture cross sections for shallow-donor centers very accurately, as shown below.

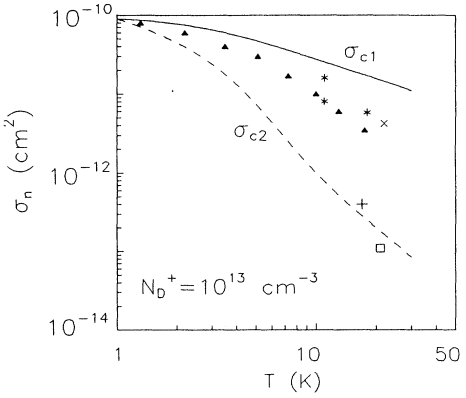

FIG. 3. Average capture cross section of donor impurities in n-type Si at equilibrium as a function of temperature. Ionized donor concentration was $N_D^+=10^{13}$ cm^{-3}. Dashed and solid lines represent simulated curves σ_{1ac} and σ_{2ac}. Symbols represent experimental data: ▲ from Ref. 10, + from Ref. 11, and □ from Ref. 12 for Si:P; * from Ref. 10 for Si:As; and × from Ref. 10 for Si:Sb.

Most of the recombinations occur in short intervals due to the strong coupling between generation-recombination processes and scattering mechanisms, which takes place in the lowest-energy region of the carrier energy-distribution function.[13] In Fig. 5, the acoustic scattering probability near the edge of the band is shown. Just below zero energy, the probability of absorption of an acoustic phonon dominates the emission, whereas

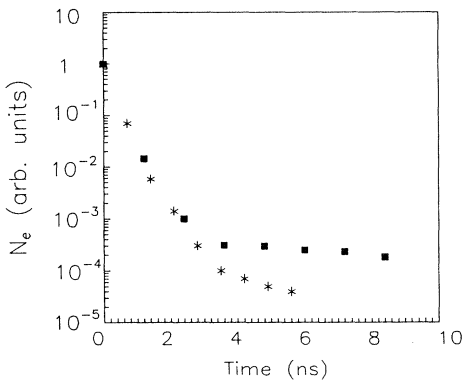

FIG. 4. Histogram of number of electrons, N_e, as a function of capture time simulated at $T=30$ K. Symbols refer to results evaluated with the Monte Carlo simulation of n-Si at equilibrium. Asterisks show case with an ionized donor concentration of 10^{14} cm^{-3} and squares correspond to $N_D^+=10^{13}$ cm^{-3}.

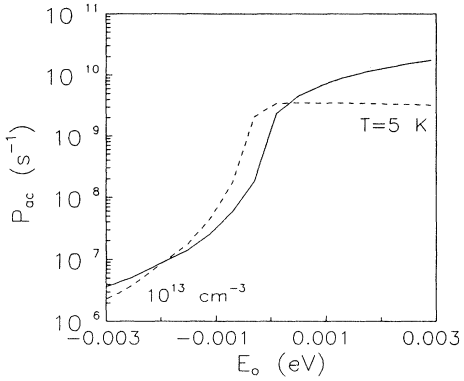

FIG. 5. Detail of Fig. 2 for the scattering rates in the region near zero energy. Solid and dashed lines are also the phonon emission and absorption rates. Here, only the $N_D^+ = 10^{13}$ cm^{-3} case is shown. These behaviors are also observed for other usual concentrations of donors. The arrow indicates the region of repetitive capture and reemission.

above this energy the opposite occurs. Therefore, as shown by the arrow in the figure, a carrier with energy near the edge of the conduction band undergoes a large number of crossings through zero energy before returning to the band or going to deeper-bound states.

We have found that the time constant associated with the short-time decay is almost independent of the donor concentration in the 10^{13} to 10^{16} cm^{-3} concentration range, in accordance with results in the literature for p-Si doping.[13] Thermal dependence has also been observed, as shown in Fig. 6. In n-Si doping, the thermal behavior of this time is also in good agreement with the energy relaxation time τ_ϵ, given by[14]

$$\tau_\epsilon = \lim_{E\to 0} \frac{\langle \epsilon \rangle - \frac{3}{2} K_B T}{e \langle v_d \rangle E} , \tag{9}$$

where $\langle \epsilon \rangle$ is the average electron energy, $\langle v_d \rangle$ is the drift velocity, and E the electric field. This agreement may suggest a certain similarity between an electron heated by an electric field, and an electron perturbed by the quasicontinuum of states produced by the Coulombic center. In both cases, the energy loss or gain for the electron is exchanged in the same way with the lattice, therefore, it is reasonable for both rates to be similar.

However, we are more interested in the time constant τ_1 associated with the long-time decay of the distribution of N_e. In our Monte Carlo simulations, the mentioned time is dependence on both shallow-donor concentration and temperature. This time, τ_1, is plotted as a function of donor concentration at several temperatures in Fig. 7. In this figure we can see that the dependence of τ_1 is inversely proportional to N_D^+. Therefore, $1/\tau_1 N_D^+$ provides a capture rate that is independent of the impurity concentration, like the behavior of experimental results. The thermal dependence of the inverse of the time associated with the long-time decay, τ_1 is shown in Fig. 8. We can also deduce that this thermal behavior is very similar to the experimental capture rate for shallow donors with a more pronounced decay with increasing temperatures.

Given the low value for the short-time decay, it is difficult to determine with traditional measurement techniques of capture cross sections. The experimental procedure carried out in Ref. 15 makes it impossible to detect the fast part of the distribution of capture times. The only possibility for observing it is with picosecond experiments. Therefore, we have admitted the capture time measured to obtain the thermal capture cross sections to be the long-time decay of the distribution of capture times. In Eq. (8) the capture time actually measured is, therefore, $\tau_c = \tau_1$. Consequently,

$$\sigma = \frac{1}{\tau_1 \langle v \rangle N_D^+} . \tag{10}$$

The temperature dependence of the average capture cross section defined by Eq. (10) is shown in Fig. 9 (solid line) and compared with available results in the literature referring to the shallow donors (P^+, As^+, and Sb^+) in silicon. To evaluate the proposed capture time, τ_1, and the mean thermal velocity, Monte Carlo simulations were performed for an ionized donor concentration, $N_D^+ = 10^{13}$

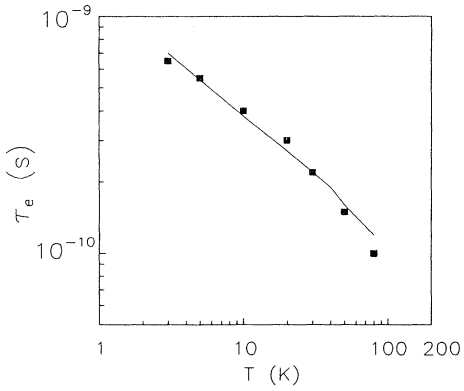

FIG. 6. Period associated with short-time decay of electron distribution as a function of temperature (symbols) calculated with Monte Carlo simulation of n-type Si at equilibrium. The line shows the thermal dependence of energy relaxation time, τ_e, also at equilibrium.

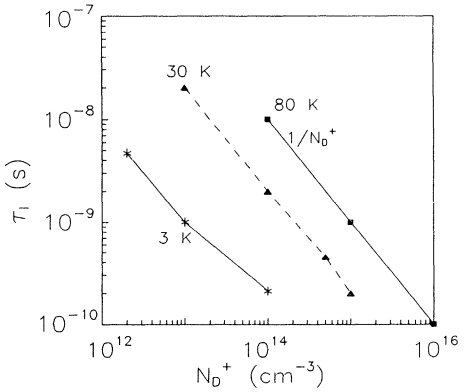

FIG. 7. Long-time decay of electron distribution as a function of ionized donor concentration obtained from Monte Carlo simulation at $T = 3$ K (asterisks), $T = 30$ K (triangles), and $T = 80$ K (squares). Lines are guides for the eye.

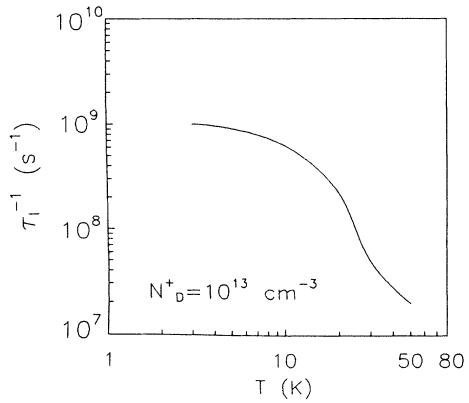

FIG. 8. Inverse of long-time decay of electron distribution as a function of temperature obtained from Monte Carlo simulation. Ionized donor concentration was 10^{13} cm^{-3}.

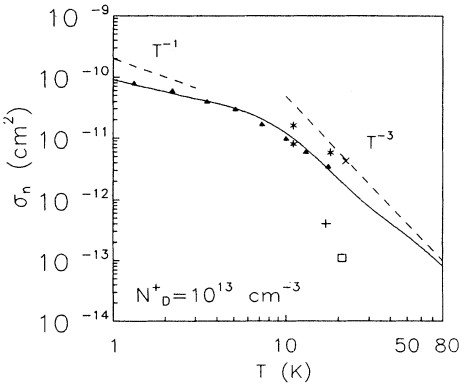

FIG. 9. Average capture cross section of donor impurities in n-type Si at equilibrium as a function of temperature. Ionized donor concentration was $N_D^+=10^{13}$ cm^{-3}. The line represents the simulated curve obtained by long-time decay of electron distribution calculated in Monte Carlo simulation. Symbols represent experimental data: ▲ from Ref. 10, + from Ref. 11, and □ from Ref. 12 for Si:P; * from Ref. 10 for Si:As; and × from Ref. 10 for Si:Sb. The asymptotic behavior analytically obtained by Ref. 3 is also shown with dashed lines.

cm^{-3}, and showed very good agreement with experimental results. The thermal dependence obtained by Abakumov *et al.*[3] in an analytical study of the cascade capture is also shown in Fig. 9 (dashed lines): T^{-1} behavior for very low temperatures and T^{-3} for higher temperatures. Our numerical results also reproduce these asymptotic behaviors.

As mentioned above, the cutoff energy E_{coff} was not a fixed parameter. To check the possible influence of this parameter, we did several simulations, varying it between $-0.5K_BT$ and $-3K_BT$. Similar results were obtained for the decay times of the electron distribution.

IV. CONCLUSIONS

Due to the nature of the Monte Carlo method, we have done a statistical study of the capture time of electrons by shallow-donor impurities. This treatment has allowed us to study the double exponential decay of the distribution of carriers as a function of their capture time and relate these decays with experimental measurements of capture cross sections.

The time constant associated with the short-time decay was in good agreement with the energy relaxation time at temperatures between 1 and 80 K. The main result was taken from the period associated with the long-time decay, τ_1. Both thermal and impurity concentration dependencies were studied for this time, τ_1. Due to the magnitude of both decay times, we have associated the long-time decay to the available capture-time measurements. To verify our consideration about the capture time, a calculation of the average capture cross section was made, extracting τ_1 from the statistical study and using it as the real capture time. We compared our numerical results with experimental data available in the literature and with a previous analytical model and found good agreement. This supports the theory that the time constant associated with the long-time decay of the histograms is a good candidate to define the measured capture time and the main importance of impurity states closest to the edge of the band in capture by cascade process.

ACKNOWLEDGMENTS

The authors are indebted to Professor L. Reggiani for his helpful discussions and suggestions throughout the course of this work.

*Fax: 34-58-243230. Electronic address: albi@gcd.ugr.es
†Electronic address: jalopez@ugr.es

[1]A. M. Stoneham, *Theory of Defects in Solids* (Clarendon, Oxford, 1975).
[2]M. Lax, Phys. Rev. **119**, 1502 (1960).
[3]V. N. Abakumov, V. I. Perel', and I. N. Yassievich, Sov. Phys. Semicond. **12**, 1 (1978).
[4]L. Reggiani, L. Varani, V. Mitin, and C. M. Van Vliet, Phys. Rev. Lett. **63**, 1094 (1989).
[5]L. Reggiani, L. Varani, and V. Mitin, Nuovo Cimento D **13**, 647 (1991).
[6]A. Palma, J. A. Jiménez-Tejada, I. Melchor, J. A. López-Villanueva, and J. E. Carceller, J. Appl. Phys. (to be published).
[7]D. A. Buchanan, M. V. Fischetti, and D. J. DiMaria, Phys. Rev. B **43**, 1471 (1991).
[8]C. Jacoboni and L. Reggiani, Rev. Mod. Phys. **55**, 645 (1983).
[9]E. Janzén, R. Stedman, G. Grossman, and H. G. Grimmeiss, Phys. Rev. B **29**, 1907 (1984).
[10]P. Norton, T. Braggins, and H. Levinstein, Phys. Rev. Lett. **30**, 488 (1973).
[11]N. S. Sacks and A. Nordbryhn, J. Appl. Phys. **50**, 6962 (1979).
[12]E. Rosencher, V. Mosser, and G. Vincent, Phys. Rev. B **29**, 1135 (1984).
[13]L. Varani, L. Reggiani, V. Mitin, C. M. Van Vliet, and T. Khun, Phys. Rev. B **48**, 4405 (1993).
[14]K. Seeger, *Semiconductor Physica. An Introduction,* 5th ed. (Springer-Verlag, Berlin, 1993).
[15]P. Norton and H. Levinstein, Phys. Rev. B **6**, 489 (1972).